ARTICLE NO. 78-1287R

Flight Investigation and Theory of Direct Side-Force Control

W. Brian Binnie*
U.S. Naval Air Training Command, Pensacola, Fla.
and
Robert F. Stengel†
Princeton University, Princeton, N.J.

Several side-force command modes were tested in Princeton's six-degree-of-freedom (6-DOF) variable-response research aircraft (VRA), emphasizing the requirements of crosswind landing and lateral offset nulling. Pilot input modes included proportional and rate thumb switch, lateral stick, and foot pedal motions to command pure lateral acceleration, pure sideslip angle, and flat-turn maneuvers. Flight test results and supporting theoretical development are presented here. It is shown that a third-order dynamic model can be used to define control surface interconnects for decoupled side-force commands. Pilots' opinions regarding desirable command modes for the landing approach were shaped by their primary flying experience, although there was consensus that side-force commands that are uncoupled from conventional control inputs are preferred.

Nomenclature

C	= interconnect gain matrix
F	= stability derivative matrix
G	= control derivative matrix
g	= acceleration due to gravity
K	= command response matrix
$K\{\ \}$	= element of K
L	= disturbance effect matrix
$L_{(\ )}$	= rolling moment stability and control derivatives
$N_{(\ )}$	= yawing moment stability and control derivatives
p	= roll rate
r	= yaw rate
u	= command input vector
V	= forward velocity
x	= state vector
$Y_{(\ )}$	= side-force stability and control derivatives
y	= lateral position
β	= sideslip angle
γ	= flight path angle
$\Delta(\ )$	= perturbation value
δ	= control surface deflection vector
δA	= aileron deflection
δP	= foot pedal deflection
δR	= rudder deflection
δS	= lateral stick deflection
δSF	= side-force control surface deflection
δY	= side-force cockpit control deflection
ϕ	= roll angle
ψ	= yaw angle

Subscripts and Superscripts

D	= desired
T	= transpose
w	= wind input
-1	= matrix inverse
2,3,4,6	= model order
*	= equilibrium value

Presented as Paper 78-1287 at the AIAA Guidance and Control Conference, Palo Alto, Calif., Aug. 7-9, 1978; revision received Jan. 15, 1979.

Index categories: Flight Operations; Guidance and Control; Handling Qualities, Stability and Control.

*Ensign, U.S. Naval Reserve; formerly, Graduate Student, Princeton University.

†Associate Professor, Department of Mechanical and Aerospace Engineering. Associate Fellow AIAA.

Introduction

AMONG the tasks of flying, the approach and landing is perhaps the most demanding for the pilot. The task is difficult to learn, and the pilot's proficiency is subject to rapid deterioration during periods when he is unable to practice the maneuver. With conventional controls, considerable skill and judgment are required to provide smooth, coordinated lateral motions. In the presence of wind disturbances, the aircraft attitude that is necessary to generate side force for path control may be awkward or undesirable, particularly at the point of touchdown. It would be helpful to have an independent means of commanding side force in this case, so that wings could be leveled, aircraft and runway centerlines could be aligned, and lateral position error could be controlled simultaneously. Alternate side-force command modes for the landing approach are the subject of this study.

Earlier research on direct side-force control (DSFC) has addressed the approach-and-landing task, and there is a growing interest in using DSFC for improved precision in weapon delivery. Extensive flight tests of DSFC modes for STOL aircraft landings were conducted in the C-131 Total In-Flight Simulator (TIFS); pilot thumb wheel inputs for manual command of pure sideslip, as well as automatic DSFC mechanizations, were investigated.[1] An off-line computer simulation illustrated the desirability of DSFC for nulling lateral offset in CTOL aircraft landings.[2] A manned simulation of STOL landings provided estimates of optimum side force-roll moment ratios; lateral offset nulling by control wheel inputs indicated the utility of lateral accelerations in the 0.2-0.3 g range.[3] Side-force control for fighter-class aircraft was first demonstrated in flight using the variable-stability T-33 aircraft,[4] while various DSFC weapon delivery modes have been investigated in ground-based simulation.[5,6] Additional flight results have been obtained from the Fighter Control-Configured Vehicle (CCV) Program.[7]

This paper reports on a theoretical and experimental investigation of DSFC during approach and landing. It begins with a review of the tasks, continues with an explanation of the dynamics of direct side-force control, and culminates with a discussion of the flight test (through touchdown) of several DSFC command modes using the variable-response research

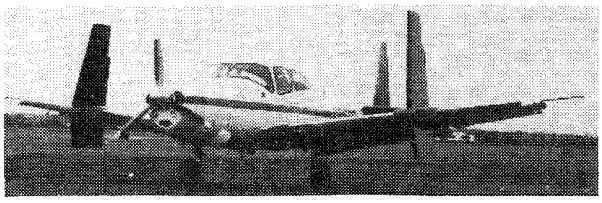

Fig. 1 The variable-response research aircraft (VRA).

aircraft (VRA), shown in Fig. 1. It is shown that there are a number of alternatives for DSFC implementation and that pilot opinion, is a strong function of the means of DSFC command, as well as the pilot's prior flight experience.

Approach-and-Landing Tasks

The principal means of counteracting side force due to crosswinds during the landing approach are "crabbing," flying with one wing low, or a combination of the two. In the crabbing approach, the wings are held level, the aircraft is yawed at zero sideslip angle to null the crosswind drift, and controls are trimmed. The aircraft's centerline and the runway are not aligned, so the pilot must "decrab" the aircraft prior to touchdown for proper alignment. In the wing-low approach, the aircraft is rolled into the wind to allow a component of the lift vector to act against the wind. This requires rudder control to maintain heading alignment and steady stick forces to counteract dihedral effect. The aircraft settles on the up-wind wheel, unless the aircraft is leveled prior to touchdown. Both methods are subject to limitations imposed by specific aircraft. For example, low-slung engine pods could limit the allowable roll attitude at touchdown, and low yaw control power (characteristic of many STOL configurations) could limit the rate of the decrab maneuver.

Even if there is negligible crosswind, lateral maneuvers prior to touchdown could be required. A lateral error normally would be corrected using an "S turn," in which the aircraft is banked to a new heading to reduce the offset, then banked in the opposite direction to re-establish the proper heading, all with zero sideslip angle.

Direct side-force control implies the ability to generate body-axis lateral accelerations that are independent of the aircraft's rolling and yawing moments. As long as there are three independent lateral-directional controls (e.g., rudder, aileron, and side-force effector), any degree of coupling or decoupling in force and moment generation can be provided by control surface interconnects.

For approach and landing the most important feature of direct side-force control is that it provides combinations of steady-state responses that cannot be obtained with conventional controls alone. For example, with the wings level, the aircraft can sideslip without yaw or yaw without sideslip. The former allows a constant-heading "sidestep," while the latter allows a flat S turn. Because there are many alternatives, several of which require crossed controls or otherwise counterintuitive pilot behavior, it is necessary to conduct flight tests to determine which DSFC modes are most attractive for the approach-and-landing task. DSFC is found to be most successful when it does not interfere with the pilot's ability to make conventional, coordinated turns.[8,9]

Dynamics of Side-Force Control

DSFC command alternatives and flight test results are put in proper perspective by first reviewing the lateral-directional equations of motion and their corresponding response characteristics. The principal distinctions between DSFC modes arise from differing quasi-steady-state responses and from the pilot actions that are necessary to achieve these conditions. Although the full set of equations is sixth order, insight can be gained by examining approximate systems, as in Ref. 10. The normally dominant response to side-force control can be approximated by a second-order model, and a third-order model provides a reasonable basis for defining manual DSFC modes. These models are applied in the discussion of flight test results that follows.

Equations of Motion

The dynamics of direct side-force control can be described by a sixth-order linear-time-invariant equation of the form

$$\Delta\dot{x}_6 = F_6\Delta x_6 + G_6\Delta\delta + L_6\Delta\beta_w \tag{1}$$

The six motion variables are contained in Δx_6,

$$\Delta x_6^T = (\Delta y \quad \Delta\psi \quad \Delta r \quad \Delta\beta \quad \Delta p \quad \Delta\phi) \tag{2}$$

the control variables are contained in $\Delta\delta$,

$$\Delta\delta^T = (\Delta\delta SF \quad \Delta\delta R \quad \Delta\delta A) \tag{3}$$

and the principal disturbance input $\Delta\beta_w$ is the sideslip angle due to crosswind. The stability derivative matrix F_6 is

$$F_6 = \left[\begin{array}{cc|cc|cc} 0 & V\cos\gamma & 0 & V & 0 & 0 \\ 0 & 0 & \sec\gamma & 0 & 0 & 0 \\ \hline 0 & 0 & N_r & N_\beta & N_p & 0 \\ 0 & 0 & (Y_r/V)-1 & Y_\beta/V & Y_p/V & (g/V)\cos\gamma \\ \hline 0 & 0 & L_r & L_\beta & L_p & 0 \\ 0 & 0 & 0 & 0 & 1 & 0 \end{array}\right] \tag{4}$$

F_6 contains stability derivatives, inertial effects, and kinematic relationships, and the disturbance effect matrix L_6 is approximated by the β derivatives of F_6. It is assumed that angles and angular rates are measured in stability axes, i.e., body axes that are nominally aligned with the velocity vector V, and that lateral position is Earth-relative. Note that F_6 is readily partitioned into nine (2×2) blocks; the three diagonal blocks represent the primary dynamics of the pure integrations for Δy and $\Delta\psi$, a reduced-order approximation for the Dutch roll mode, and a reduced-order approximation for the roll and spiral modes. The off-diagonal blocks provide coupling between the modes. The classical Dutch roll, roll, and spiral modes govern Δr, $\Delta\beta$, Δp, and $\Delta\phi$, and they are unaffected by Δy and $\Delta\psi$. Consequently, these modes are completely defined by the lower right (4×4) block of Eq. (4). With negligible Y_r and Y_p, as well as $\gamma \simeq 1$, this is

$$F_4 = \begin{bmatrix} N_r & N_\beta & N_p & 0 \\ -1 & Y_\beta/V & 0 & g/V \\ L_r & L_\beta & L_p & 0 \\ 0 & 0 & 1 & 0 \end{bmatrix} \tag{5}$$

L_4 is approximated by the second column of F_4, and the corresponding control effect matrix G_4 is

$$G_4 = \left[\begin{array}{ccc} N_{\delta SF} & N_{\delta R} & N_{\delta A} \\ Y_{\delta SF}/V & Y_{\delta R}/V & Y_{\delta A}/V \\ L_{\delta SF} & L_{\delta R} & L_{\delta A} \\ \hline 0 & 0 & 0 \end{array}\right] = \left[\begin{array}{c} G_3 \\ \hline 0\ 0\ 0 \end{array}\right] \quad (6)$$

The control effect matrix contains a nonsingular (3×3) block G_3 and a row of zeros. Defining the cockpit command inputs as

$$\Delta u^T = (\Delta\delta Y \quad \Delta\delta P \quad \Delta\delta S) \quad (7)$$

any desired force/moment generation characteristic G_{3_D} can be provided by implementing the appropriate control surface interconnect gain matrix C between the cockpit controls and control surfaces. Neglecting actuation lags,

$$\Delta\delta = C\Delta u \quad (8)$$

where

$$C = G_3^{-1} G_{3_D} \quad (9)$$

The fourth-order dynamic model is then

$$\Delta\dot{x}_4 = F_4\Delta x_4 + G_{4_D}\Delta u + L_4\Delta\beta_w \quad (10)$$

where G_{4_D} is defined as in Eq. (6).

Constant steady-state response to constant command inputs and disturbances is defined by $\Delta\dot{x}=0$; if this equilibrium condition exists, the solution of Eq. (10) is

$$\Delta x_4^* = -F_4^{-1}(G_{4_D}\Delta u^* + L_4\Delta\beta_w^*) \quad (11)$$

where $(\ )^*$ indicates the equilibrium value. F must be nonsingular for nontrivial values of Δx^* to exist; if F is singular, one or more modes of F are pure integrations, and the corresponding motion variables do not have constant equilibrium values. The equilibrium values of the remaining variables then can be found by reducing the order of Eq. (11) to eliminate the unbounded response. If F is stable, "equilibrium" is synonymous with "steady-state"; if not, Eq. (11) still defines an equilibrium point, but the aircraft's natural stability must be augmented to achieve a steady state.

The equilibrium controls necessary to null response to a constant crosswind $\Delta\beta_w^*$ are found by setting $\Delta x_4^* = 0$. Crosswind forcing is nulled by

$$\Delta u^* = -G_{3_D}^{-1} L_3 \Delta\beta_w^* \quad (12)$$

where G_{3_D} and L_3 are the top three rows of G_{4_D} and L_4.

Steady-State Response to Control

The previous section defines the aircraft's steady-state response to constant inputs; this section illustrates that there are three quasi-steady-state solutions of possible interest, corresponding to second-, third-, and fourth-order models of lateral-directional dynamics and DSFC control.

A second-order yaw mode approximation illustrates the aircraft's basic side-force response; it is derived from the first two rows of Eq. (11), assuming that the wings are held level by independent roll control:

$$\left[\begin{array}{c} \Delta\dot{r} \\ \Delta\dot{\beta} \end{array}\right] = \left[\begin{array}{cc} N_r & N_\beta \\ -1 & Y_\beta/V \end{array}\right]\left[\begin{array}{c} \Delta r \\ \Delta\beta \end{array}\right] + \left[\begin{array}{cc} N_{\delta Y} & N_{\delta P} \\ Y_{\delta Y}/V & Y_{\delta P}/V \end{array}\right]\left[\begin{array}{c} \Delta\delta Y \\ \Delta\delta P \end{array}\right] \quad (13a)$$

or

$$\Delta\dot{x}_2 = F_2\Delta x_2 + G_{2_D}\Delta u_2 \quad (13b)$$

Desired control effects are defined by the product of the natural control effects and an interconnect gain matrix [as in Eq. (9)]. Assume first that $N_{\delta Y}=0$ and $Y_{\delta P}=0$, i.e., that the side-force controller and foot pedals command pure side force and yaw moment, respectively. Then, from

$$\Delta x_2^* = -F_2^{-1} G_{D_2}\Delta u^* \quad (14)$$

the steady-state yaw rate and sideslip angle are

$$\Delta r^* = \frac{N_\beta Y_{\delta Y}\Delta\delta Y^* - Y_\beta N_{\delta P}\Delta\delta P^*}{VN_\beta + N_r Y_\beta} \quad (15)$$

and

$$\Delta\beta^* = \frac{-(N_r Y_{\delta Y}\Delta\delta Y^* + N_{\delta P}\Delta\delta P^*)}{VN_\beta + N_r Y_\beta} \quad (16)$$

These equations illustrate that, in general, uncoupled control forces and moments produce coupled motion variable response.

It follows that suitable values of $N_{\delta Y}$ and $Y_{\delta P}$ could be found to provide decoupled steady-state control. By substitution in Eqs. (15) and (16), it can be seen that if

$$N_{\delta Y}/Y_{\delta Y} = -N_r/V \quad (17)$$

then $\Delta\delta Y^*$ would have zero effect on $\Delta\beta^*$. Similarly, if

$$N_{\delta P}/Y_{\delta P} = N_\beta/Y_\beta \quad (18)$$

then $\Delta\delta P^*$ has zero effect on Δr^*. In this example, the $\Delta\delta Y$ cockpit control would command yaw rate alone, and the foot pedals would command sideslip angle alone, subject to Dutch roll transient responses in both variables.

Repeating this process for the fourth-order lateral-directional model [Eq. (10)] allows rolling effects to be considered, but it introduces some apparently curious effects of DSFC: Whereas the side force produced by $\Delta\delta Y^*$ has a strong effect on the Δr^* and $\Delta\beta^*$ predicted by the second-order model, it has no effect on these variables in the fourth-order model. In fact, the only effect of $Y_{\delta Y}\Delta\delta Y^*$ is on steady-state roll angle. Defining the desired control effect matrix to produce pure side force and moments,

$$G_{4_D} = \left[\begin{array}{ccc} 0 & N_{\delta P} & 0 \\ Y_{\delta Y}/V & 0 & 0 \\ 0 & 0 & L_{\delta S} \\ 0 & 0 & 0 \end{array}\right] \quad (19)$$

and evaluating Eq. (11) (with $\Delta\beta_w=0$) leads to the following steady-state relationships:

$$\Delta r^* = \frac{-(L_\beta N_{\delta P}\Delta\delta P^* - N_\beta L_{\delta S}\Delta\delta S^*)}{L_\beta N_r - L_r N_\beta} \quad (20)$$

$$\Delta\beta^* = \frac{L_r N_{\delta P}\Delta\delta P^* - N_r L_{\delta S}\Delta\delta S^*}{L_\beta N_r - L_r N_\beta} \quad (21)$$

$$\Delta p^* = 0 \tag{22}$$

$$\Delta\phi^* = \frac{Y_{\delta Y}}{g}\Delta\delta Y^* + \frac{(L_\beta + L_r Y_\beta/V)N_{\delta P}}{(g/V)(L_\beta N_r - L_r N_\beta)}\Delta\delta P^* + L_{\delta S}\Delta\delta S^* \tag{23}$$

These equations represent the steady-state values on the time scale of the spiral mode, whose time constant (stable or unstable) may vary from several seconds to infinity. In the latter case, the corresponding eigenvalue is zero, F_4 becomes singular, and the fourth-order steady-state equations break down.

Long-period spiral mode dynamics tend to obscure the shorter term quasi-steady-state effects of DSFC that are most apparent to the pilot, and it is suggested that a more useful model for investigating DSFC is formed by the third-order approximation, which includes the Dutch roll and roll modes and is exact for a neutral spiral mode. Truncating F_4 and G_{4_D} to eliminate $\Delta\phi$, the third-order equivalent of Eq. (11), with G_{3_D} defined by the first three rows of Eq. (19), is

$$\begin{bmatrix} \Delta r^* \\ \Delta\beta^* \\ \Delta p^* \end{bmatrix} = \frac{\begin{bmatrix} (L_p N_\beta - L_\beta N_p)Y_{\delta Y}/V & -(L_p Y_\beta/V)N_{\delta P} & (N_p Y_\beta/V)L_{\delta S} \\ (L_r N_p - L_p N_r)Y_{\delta Y}/V & -L_p N_{\delta P} & N_p L_{\delta S} \\ (L_\beta N_r - L_r N_\beta)Y_{\delta Y}/V & (L_\beta + L_r Y_\beta/V)N_{\delta P} & -(N_\beta + N_r Y_\beta/V)L_{\delta S} \end{bmatrix}}{L_p(N_\beta + N_r Y_\beta/V) - N_p(L_\beta + L_r Y_\beta/V)} \begin{bmatrix} \Delta\delta Y^* \\ \Delta\delta P^* \\ \Delta\delta S^* \end{bmatrix} \tag{24}$$

The steady-state values predicted by Eq. (24) occur on the time scale of the Dutch roll and roll modes (a few seconds or less). The equation illustrates again that uncoupled force and moment generation does not provide uncoupled response to controls. Suppose that the desired decoupled steady-state response is

$$\begin{bmatrix} \Delta r^* \\ \Delta\beta^* \\ \Delta p^* \end{bmatrix} = \begin{bmatrix} K^r_{\delta Y} & 0 & 0 \\ 0 & K^\beta_{\delta P} & 0 \\ 0 & 0 & K^p_{\delta S} \end{bmatrix} \begin{bmatrix} \Delta\delta Y^* \\ \Delta\delta P^* \\ \Delta\delta S^* \end{bmatrix} \tag{25a}$$

or

$$\Delta x_3^* = K_3 \Delta u^* \tag{25b}$$

where the diagonal elements represent the desired scalar responses (e.g., degree per second per inch of stick). Then

$$K_3 = -F_3^{-1} G_{3_D} \tag{26}$$

$$G_{3_D} = -F_3 K_3 \tag{27}$$

and the interconnect gain matrix [Eq. (9)] is

$$C = -G_3^{-1} F_3 K_3 \tag{28}$$

Equation (28) provides a simple means of designing control interconnects for alternate DSFC and angular control modes that possess quasi-steady-state response specified by Eq. (25).

Transient Response to Control

The VRA's transient response to step control inputs has been computed by digital integration of Eq. (10) with stability and control derivatives defined in Table 1. At its approach airspeed of 75 knots, the aircraft's Dutch roll period and damping ratios are 3.2s and 0.24, respectively, the stable roll mode time constant is 0.2 s, and the unstable spiral mode constant is 112 s. The flying qualities parameter ϕ/β, which is the magnitude ratio of the roll and sideslip angle components of the Dutch roll eigenvector, is 0.72. Consequently, the time histories of VRA response evidence lightly damped yaw oscillations with relatively low coupling into roll motions, moderate roll response to control with negligible Dutch roll excitation, and a very long period path divergence. The following two figures assume that VRA interconnects are adjusted to provide pure side force from $\Delta\delta Y$, pure yaw moment from $\Delta\delta P$, and pure roll moment from $\Delta\delta S$.

Figure 2 illustrates the aircraft's response to a unit side force (normalized to $\Delta\delta SF = 1$ deg). Yaw rate and sideslip responses have the same sense, indicating that the nose is left of the velocity vector for right yaw rate. Roll response is minimal, and the Dutch roll transient takes about 8 s to die out. Thus, side force alone commands an uncoordinated wings-level turn.

A unit yaw moment (normalized to $\Delta\delta R = 1$ deg) provides responses of somewhat higher magnitude, with Δr and $\Delta\beta$ of opposite sign (Fig. 3). The balance of L_β, L_r, and L_p causes a steady roll rate, and the roll angle grows to a large value. The ailerons could be used in conventional fashion to coordinate the turn or in opposition to the rudder to maintain heading with nonzero sideslip and roll angles.

With the third-order steady-state interconnects described by Eqs. (24) and (28), substantially different responses are obtained, although modal characteristics are unchanged. Defining K_3 as an identity matrix [Eq. (25)], the desired control effect matrix [Eq. (27)] takes the following values:

$$G_{3_D} = \begin{bmatrix} 0.685 & -3 & 0.199 \\ 1 & 0.315 & 0 \\ -1.6 & 6.096 & 4.6 \end{bmatrix} \tag{29}$$

i.e., G_{3_D} is $-F_3$. A unit $\Delta\delta Y$ command then provides the response shown in Fig. 4. The figure illustrates that Δr approaches a short-term "steady-state" value of about 0.9 deg/s, while $\Delta\beta$ and Δp approach zero following the initial transient. The 10% "hangoff" in Δr can be attributed to the steady roll angle of 0.4 deg, which is initiated by the Δp transient and is unmodeled in the interconnect equation. Otherwise, this is very nearly a wings-level turn.

A unit $\Delta\delta P$ command results in a "steady-state" sideslip angle of 1 deg, while Δr, Δp, and $\Delta\phi$ all approach zero (Fig. 5). There is a large Δr transient corresponding to the $\Delta\beta$ buildup, and this mode is seen to provide a "sidestep" maneuver with negligible heading change.

DSFC Flight Testing

DSFC flight testing allowed pure side-force control, as represented by Fig. 2, to be compared with control modes that blended side force with rolling and yawing moments to yield

Table 1 VRA lateral-directional model for 75-knot airspeed (angles and control deflections in radians)

N_r	$= -0.685$	L_r	$= 1.6$	Y_β/V	$= -0.315$
N_β	$= 3$	L_β	$= -6.096$	g/V	$= 0.254$
N_p	$= -0.199$	L_p	$= -4.6$	$Y_{\delta SF}/V$	$= 0.25$
$N_{\delta A}$	$= -1.09$	$L_{\delta R}$	$= 0.392$	$N_{\delta SF}$	$= 1.54$
$N_{\delta R}$	$= -4.12$	$L_{\delta A}$	$= 11.4$		

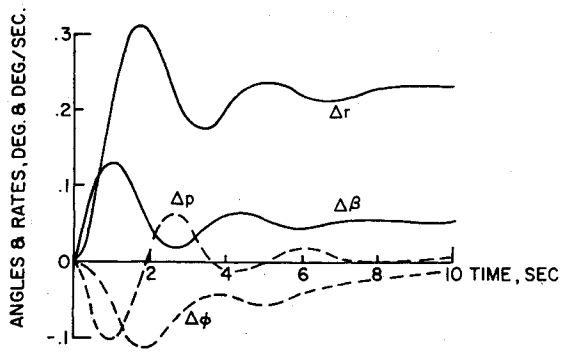

Fig. 2 VRA response to a unit step side force.

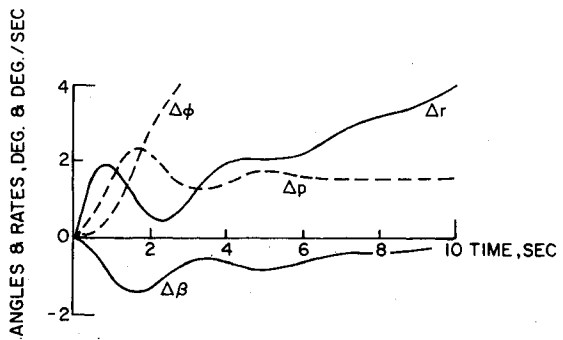

Fig. 3 VRA response to a unit step yaw moment.

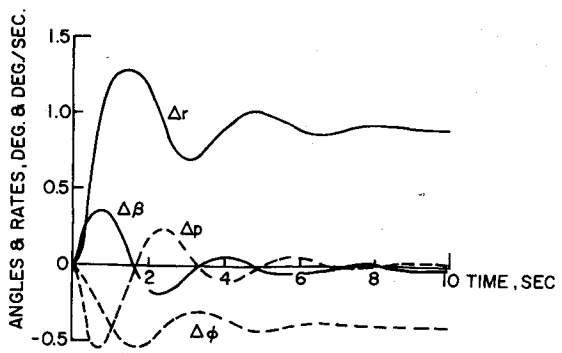

Fig. 4 VRA step response with third-order steady-state yaw rate interconnects.

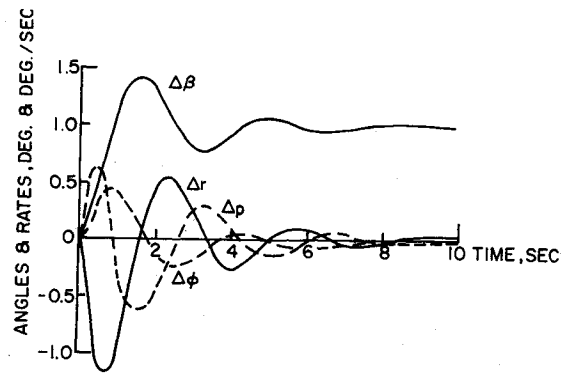

Fig. 5 VRA step response with third-order steady-state sideslip angle interconnects.

response characteristics similar to those in Figs. 4 and 5. Details of the flight test aircraft (Fig. 1) are contained in the Appendix.

The four basic command modes are most readily described in terms of their associated desired control effects matrices G_{3_D}. For the separate DSFC mode (mode 1),

$$G_{3_D} = \begin{bmatrix} 0 & N_{\delta R} & 0 \\ Y_{\delta Y}/V & 0 & 0 \\ 0 & 0 & L_{\delta A} \end{bmatrix} \tag{30}$$

i.e., foot pedal and lateral stick sensitivities are set to the aircraft's nominal values and a variable gain ($Y_{\delta Y}/V$) is assigned to a thumb switch. (For mode 1A, thumb-lever input provides proportional deflection of the side-force panels. For mode 1B, a thumb trim switch commands a discrete side-force panel rate.) The side force-yaw mode (mode 2) is represented by

$$G_{3_D} = \begin{bmatrix} 0 & N_{\delta R} & 0 \\ 0 & Y_{\delta P}/V & 0 \\ 0 & 0 & L_{\delta A} \end{bmatrix} \tag{31}$$

Foot pedals command either sideslip angle (2A) or yaw rate (2B), with lateral stick inputs being used to hold wings level. The side force-roll mode (mode 3) is represented by

$$G_{3_D} = \begin{bmatrix} 0 & N_{\delta R} & 0 \\ 0 & 0 & Y_{\delta S}/V \\ 0 & 0 & L_{\delta A} \end{bmatrix} \tag{32}$$

Here, the side-force panels augment the lateral acceleration produced by roll (as in Ref 3), and the rudder is used to coordinate the maneuver. Mode 4 is a dual-interconnect mode combining Eqs. (31) and (32). None of these modes duplicates exactly the third-order decoupling conditions of Eq. (25), although pure sideslips and yaw rates can be commanded by multiple pilot control inputs when appropriate values of $Y_{\delta Y}$, $Y_{\delta P}$, and $Y_{\delta S}$ are chosen. Each G_{3_D} specifies a C [Eq. (9)], which is used to implement the command mode. During flight testing, these side-force sensitivities were chosen by each evaluation pilot to produce the "best" response in his judgment.

VRA flight tests were preceded by a rudimentary fixed-base simulation of VRA lateral-directional dynamics. The simulation consisted of a control stick, foot pedals, oscilloscope display of bank angle and lateral position, heading angle meter, and analog computer. Each DSFC mode was "flown" by the project's evaluation pilots prior to flight, and the simulation was used to aid postflight analysis as well.

Testing Procedures

Each configuration was introduced to the evaluation pilot at altitude prior to actual approaches and landings. This allowed the pilot to examine the aircraft's response in various maneuvers and in some cases to adjust the scaling of side-force control to his preference. Each evaluation pilot performed at least four approaches and landings with each DSFC mode.

All four DSFC configurations were tested in instrument approach using a TALAR fixed-beam microwave landing system (MLS) for manual guidance, as well as in visual approach. The majority of test flights were made without stability augmentation, although the proportional thumb lever and side force-roll modes also were tested with roll- and yaw-attitude-hold control loops.

The flight path used for experimentation is shown in Fig. 6. All approaches included the final offset maneuver; individual runs varied according to approach guidance type (visual or MLS) and disturbance environment (calm, simulated crosswind, or simulated turbulence). The evaluation pilot

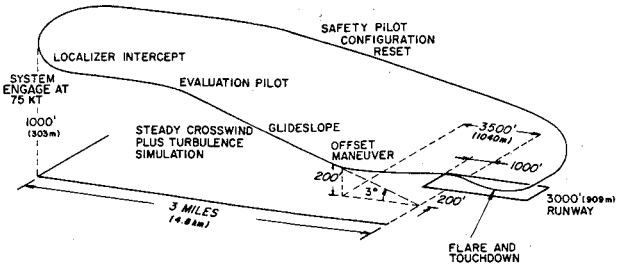

Fig. 6 Flight path for DSFC experimentation.

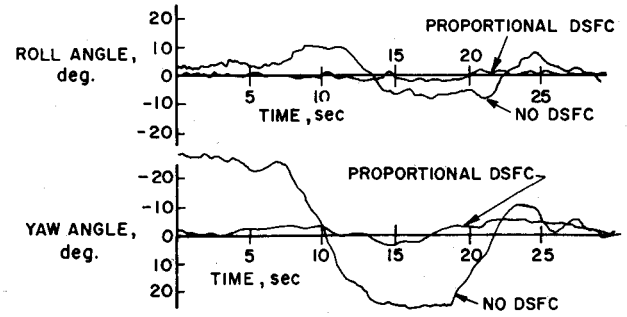

Fig. 7 Flight test comparison of bank and heading angles with proportional DSFC (mode 1A) and no DSFC.

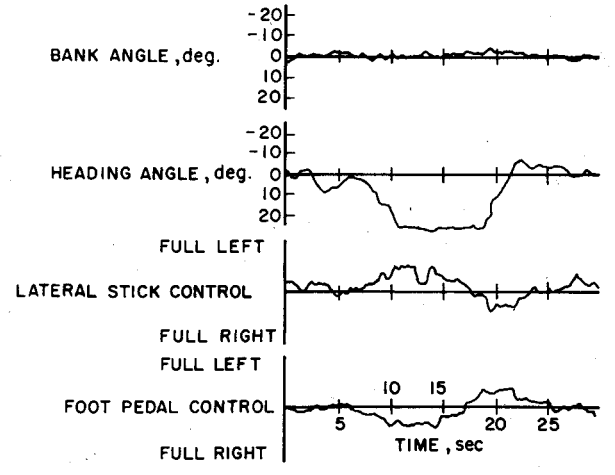

Fig. 8 Typical approach with flat-turn DSFC mode (mode 2B).

assumed control of the aircraft about three miles (5 km) from touchdown, flew the approach and landing, maintained rollout control, accelerated to rotation speed, and completed the takeoff prior to the next run. The offset maneuver was initiated at 200-ft (61-m) altitude, about 2500 ft (760 m) from touchdown. Without DSFC, the S-turn offset maneuver required brisk, but not extreme, control usage.

Cooper-Harper pilot ratings[11] were assigned to each mode by the evaluation pilot, and both pilots provided commentary. Control modes were rated separately for approach, landing, takeoff, and turn coordination, with nominal turbulence and crosswind in the first three cases and without disturbances (at altitude) for the fourth. Simulated turbulence was "light to moderate" (3 fps − 1 m/s rms) with 1000-ft (305-m) scale length, while the simulated crosswind was 16 knots (8.2 m/s), equivalent to a 12-deg crab angle at the landing speed. With actual crosswind, the latter value increased to a 25-knot (13-m/s) maximum.

Without DSFC, the VRA's calm-air approach and turn coordination characteristics were given pilot ratings of 2 (good, negligible deficiencies). In turbulence, approach and landing ratings decreased to 3.5, while the takeoff was rated as 3 (fair, mildly unpleasant deficiencies).

Flight Test Results

Separate DSFC Mode (Mode 1)

The distinguishing feature of both thumb-lever proportional command and trim switch rate command of δSF is that they offer independent side-force control. The stick and pedals provide conventional responses, so DSFC requires a minimum of readjustment in piloting style. The performance of the two separate DSFC modes was accurately forecast by fixed-base simulation, which indicated that separate DSFC is easy to fly and effective in controlling lateral translation.

Proportional command (mode 1A) clearly was preferred over the rate command mode, primarily because the response was predictable and the side-force panels returned to center when the thumb lever was released. Takeoff and turn coordination ratings were unaffected by DSFC, but approach-and-landing pilot ratings improved to 2.5-3 in this mode, with thumb-lever gain adjusted to provide maximum available side acceleration (0.25 g) with full thumb-lever throw [about ± 1 in. (± 2.5 cm)]. Ratings improved by a half point with roll attitude hold. The principal complaint was that the hand had to be stretched too much in thumb-lever actuation, particularly when the microphone trigger switch on the control stick was being keyed simultaneously; however, the sense of control was natural, and little trouble was experienced in using the stick and rudder to counter transients induced by turbulence or DSFC inputs.

Figure 7 compares the bank and heading angles experienced with this command mode to the non-DSFC command mode during the lateral-offset maneuver under conditions of simulated crosswind and turbulence. The former allowed ϕ and ψ to be held within ± 5 deg, while bank and heading angle excursions with the latter were 10 and 25 deg, respectively.

Reaction to the δSF rate command (mode 1B) was less favorable because of the difficulty in nulling side-force panel deflection. Although the pilot could refer to a panel meter to center the surfaces, he was unwilling to devote attention to this task during landing; hence, there normally was a residual side-force bias which the pilot nulled by roll control. Pilot ratings for approach and landing degenerated to 4.5-5 as a result. Nevertheless, it is felt that rate command could be an attractive DSFC mode if the centering problem was solved by a deflection "washout" or reset mechanism.

Roll and yaw attitude hold encouraged liberal use of DSFC by both pilots. Pilot A, whose background was in military flying, consistently preferred more rapid correction of lateral offsets than pilot B, whose background was in general aviation; he often used the full amount of available side force (0.25 g) during the crosswind landing.

Side Force-Yaw Mode (Mode 2)

Both steady sideslip and flat-turn foot pedal command modes were tested, and while the two pilots agreed on the relative merits of the modes, they weighed these features differently. Pilot A preferred the "snappy" yaw response of the flat-turn mode (mode 2B), while Pilot B preferred the wings-level sideslip mode (mode 2A). The advantage of the former mode is that it allows more rapid offset nulling at the expense of turning off the runway heading. The latter permits crosswind and offset correction while maintaining runway heading. Nevertheless, neither of these modes was rated as highly as separate DSFC or no DSFC at all. The flat-turn mode received pilot ratings of 4.5-5 for approach, landing, and takeoff, with turn coordination rated at 3.5. The steady sideslip mode was rated 4 for approach and turn coordination, 5 for landing, and 5.5 for takeoff.

In the flat-turn mode ($Y_{\delta P}/V = -0.43$), there is a tendency to accentuate crosswind effects during final runway alignment. The foot pedal input which aligns aircraft and runway

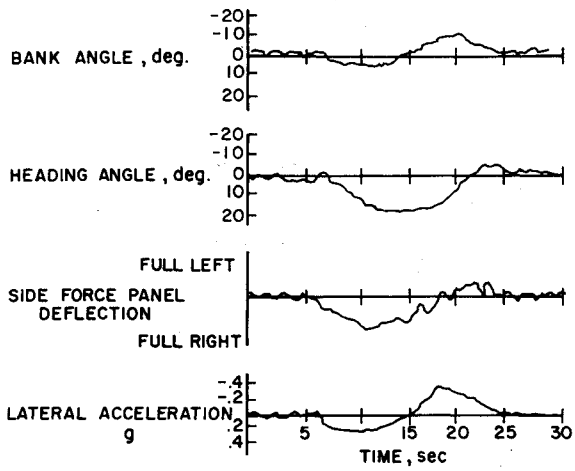

Fig. 9 Representative time history for the side-force roll mode (mode 3).

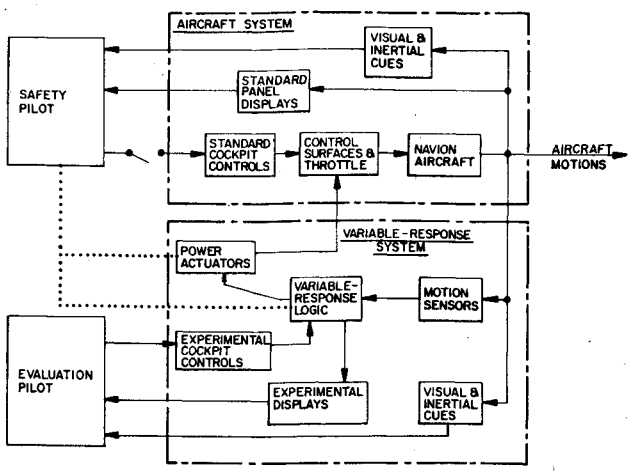

Fig. 10 Overview of the VRA experimental system.

centerlines also produces a side force that increases lateral drift. Considerable bank angle is required to cancel the drift, and the flare maneuver becomes more demanding than usual. Figure 8 illustrates the angles and cockpit control deflections required for crosswind approach with the flat-turn mode. Wing are held near level; there are large and rapid heading changes, and crossed controls are required, both of which contribute to the pilot opinions of deficient control.

The main difficulty with foot pedal command of steady sideslip ($Y_{\delta P}/V = 6.02$) is possible confusion about control usage near the ground. Conventional roll and yaw controls produce lateral displacement which is opposite to conventional response, leading to mismatched control activity. This mismatch is especially critical at touchdown or liftoff, as the aircraft's response to pedal steering commands changes sign abruptly. On the ground with nose-wheel steering, right pedal produces right yaw, leading to right translation; at rotation and beyond, right pedal commands left translation.

Side Force-Roll Mode (Mode 3)

Steady sideslip command via lateral stick ($Y_{\delta S}/V = 0.62$) received mixed reviews from the evaluation pilots. Pilot A considered the aircraft response too slow, he disliked the bank angle transient required to initiate lateral motions, and he felt that controlling against the crosswind interfered with precise pitch control for flare. Pilot B preferred this mode to the foot pedal DSFC mode, considering it beneficial to hold heading with the pedals and to adjust lateral offset with the stick. He felt that problems with the roll transient could be avoided by taking care to use smooth control inputs. Both pilots found it tiring to hold control against a stiff crosswind, and they considered the lack of independent roll control unfavorable. Attempts to correct lateral upsets in turbulence excited undue lateral motions, and turn entries were hard to coordinate. Accordingly, the pilot rating for turn coordination was 4.5-5, while ratings for approach, landing, and takeoff were 3.5. With roll and yaw attitude hold, the stick was effectively turned into an independent side-force controller. This mode was rated at 2.5 for the approach and landing.

Figure 9 illustrates typical aircraft angles and levels of side force used in this mode (without roll attitude hold). By comparison with separate DSFC (Fig. 7), angle excursions are large—in fact, they are comparable to excursions with conventional control. Heading angle changes are less than those experienced with the flat-turn mode (Fig. 8), but roll angles are larger.

Dual-Interconnect Mode (Mode 4)

Contrary to expectations derived from pilot-aircraft analysis and ground simulation, commanding wings-level sideslip with both $Y_{\delta P}$ and $Y_{\delta S}$ interconnects did not improve pilot ratings of DSFC. As implied by earlier results, an infinite number of dual-interconnect pairs could provide sideslip command with zero heading rate. For the flight tests, only positive values of $Y_{\delta P}$ and $Y_{\delta S}$ were considered, and increases in one parameter were accompanied by increases in the other. Given free choice, pilot A selected high side-force values, and pilot B selected low values; however, neither pilot was impressed with the dual mode, their impressions being that the cockpit became "too busy," especially in turbulence. The dual-mode approach was rated at 3, the landing at 4, and the takeoff and turn coordination at 4.5.

Flight Test Summary

Separate side-force command with proportional thumb lever was the preferred DSFC mode derived from these flight tests, and it contributed to improved approach-and-landing pilot ratings for the research aircraft. Roll attitude hold provided further improvement in pilot opinion. Separate rate command did not provide self-centering of the side-force panels, and the resulting side-force bias led to excessive roll control at touchdown. Integrated side force-roll control produced pilot ratings that were similar to the VRA's ratings without DSFC; adding roll attitude hold converted the stick to a separate side-force controller and improved the ratings. Integrated side force-yaw control possessed some interesting features, but the net effect was degraded pilot ratings. The dual modes considered did not provide improvement. The maximum available side force (0.25 g) appeared more than adequate for the DSFC modes tested, with typical levels of 0.1 to 0.2 g being used for crosswind and offset correction in this study.

Conclusion

This paper has presented results of a theoretical and experimental investigation of direct side-force control for aircraft approach and landing. Linear analysis indicates that a second-order model provides insights regarding alternative applications of DSFC, a third-order model is most useful for characterizing the desired quasi-steady-state response to control and defining DSFC command modes, and a fourth-order model is appropriate for investigating transient response and long-term equilibrium. Flight testing with the VRA leads to the conclusion that pilots generally prefer direct side-force command modes that are separate from the conventional stick and pedal inputs, as this interferes least with learned patterns of piloting behavior and provides the greatest degree of independent flight path control.

The flight test program concentrated on open-loop DSFC command modes, although limited testing in conjunction with

roll- and yaw-attitude-hold modes demonstrated that further improvements can be expected from closed-loop DSFC. Areas for future research include flight testing of decoupled DSFC modes [as in Eq (25)], quantitative investigations of pilot work load and path-following error using DSFC, and practical methods of generating the necessary side force [some of which are suggested in Ref. 2]. This program has demonstrated that direct side-force control provides improved approach-and-landing control with large crosswinds and initial lateral offsets.

Appendix: Variable-Response Research Aircraft (VRA)

The flight test aircraft (Fig. 1) is a highly modified Navion, equipped with motion sensors, control surface actuators, up-and-down flaps, and side-force panels. For the DSFC program, control logic, interconnects, and feedback paths were implemented with analog circuitry. The general arrangement of VRA systems is shown in Fig. 10. The conventional mechanical aircraft system is flown by the safety pilot, while the fly-by-wire aircraft system used for research is flown by the evaluation pilot. This system includes redundant aileron, elevator, and side-force actuators for protection against system failures. The evaluation pilot's station is tailored to the experiment; for the DSFC program, this station included a center control stick, thumb switches for two DSFC modes, rudder pedals, sideslip and side-force-panel meters, and conventional instruments. The safety pilot is the in-flight test conductor, monitoring systems and adjusting all experimental parameters. The pilot has several electrical and hydraulic mechanisms for disengaging the variable-response system in the event of a malfunction, as well as an "automatic go-around" abort mode, which makes safe experimentation through touchdown possible.

Acknowledgments

This work was supported under Contract No. 18.884/SAT.2/LL, Office National d'Etudes et de Recherches Aerospatiales. E. Seckel initiated the research, and D. R. Ellis was instrumental in flight test planning and operations.

References

[1] Boothe, E.M. and Ledder, H.J., "Direct Side Force Control for STOL Crosswind Landings," *Journal of Aircraft,* Vol. 11, Oct. 1974, pp. 631-638.

[2] Mercier, D. and Duffy, R., "Application of Direct Side-Force Control to Commercial Transport," AIAA Paper 73-886, Key Biscayne, Fla., Aug. 1973.

[3] Jenkins, H.W.M., "Direct Sideforce Control for STOL Transport Aircraft," AIAA Paper 73-887, Key Biscayne, Fla., Aug. 1973.

[4] Hall, G.W., "A Flight Test Investigation of Direct Side-Force Control," AIAA Paper 72-94, San Diego, Calif., Jan. 1972.

[5] Carlson, E.F., "Direct Sideforce Control for Improved Weapon Delivery Accuracy," AIAA Paper 74-70, Washington, D.C., Aug. 1974.

[6] Brulle, R.V., "Dive Bombing Simulation Results Using Direct Side Force Control Modes," AIAA Paper 77-1118, Hollywood, Fla., Aug. 1977.

[7] Watson, J.H. and McAllister, J.D., "Direct-Force Flight-Path Control – The New Way to Fly," AIAA Paper 77-1119, Hollywood, Fla., Aug. 1977.

[8] Binnie, W.B., "Direct Side Force Control – A Flight Investigation of Handling Qualities during Terminal Area Operations," M.S.E. Thesis, Princeton Univ., Princeton, N.J., Jan. 1978.

[9] LaBurthe, C.L., Petit, J.P., and Guillard, A., "Use of Direct Forces – Predictions and Flight Tests on a Light 6 Axes Variable Stability Aircraft of Princeton University," presented at AGARD Symposium of Stability and Control, Ottawa, Canada, Sept. 1978.

[10] Ashkenas, I. and McRuer, D.T., "Approximate Airframe Transfer Functions and Application to Single Sensor Control Systems," WADC-TR-58-82, June 1958.

[11] Harper, R.P., Jr. and Cooper, G.E., "The Use of Pilot Rating in the Evaluation of Aircraft Handling Qualities," NASA TN D-5153, April 1969.